

# Electrochemical Capture and Release of Carbon Dioxide Using a Disulfide–Thiocarbonate Redox Cycle

Poonam Singh,<sup>†</sup> Joseph H. Rheinhardt,<sup>†</sup> Jarred Z. Olson,<sup>‡</sup> Pilarisetty Tarakeshwar,<sup>†</sup> Vladimiro Mujica,<sup>†</sup> and Daniel A. Buttry<sup>\*,†,§</sup>

<sup>†</sup>School of Molecular Sciences, Arizona State University, Tempe, Arizona 85281, United States

<sup>‡</sup>Department of Chemistry, University of Washington, Seattle, Washington 98105, United States

## S Supporting Information

**ABSTRACT:** We describe a new electrochemical cycle that enables capture and release of carbon dioxide. The capture agent is benzylthiolate ( $RS^-$ ), generated electrochemically by reduction of benzyl disulfide (RSSR). Reaction of  $RS^-$  with  $CO_2$  produces a terminal, sulfur-bound monothiocarbonate,  $RSCO_2^-$ , which acts as the  $CO_2$  carrier species, much the same as a carbamate serves as the  $CO_2$  carrier for amine-based capture strategies. Oxidation of the thiocarbonate releases  $CO_2$  and regenerates RSSR. The newly reported *S*-benzylthiocarbonate (IUPAC name benzylsulfanylformate) is characterized by  $^1H$  and  $^{13}C$  NMR, FTIR, and electrochemical analysis. The capture–release cycle is studied in the ionic liquid 1-butyl-1-methylpyrrolidinium bis(trifluoromethylsulfonyl)imide (BMP TFSI) and dimethylformamide. Quantum chemical calculations give a binding energy of  $CO_2$  to benzyl thiolate of  $-66.3 \text{ kJ mol}^{-1}$ , consistent with the experimental observation of formation of a stable  $CO_2$  adduct. The data described here represent the first report of electrochemical behavior of a sulfur-bound terminal thiocarbonate.

Climate impacts from high atmospheric  $CO_2$  concentrations due to carbon-based fuel combustion continue to drive high levels of research activity in carbon capture and sequestration (CCS).<sup>1</sup> A number of approaches have been described for carbon capture, both at point sources such as power plants (postcombustion  $CO_2$  capture) and directly from the atmosphere (direct air capture). Many of these approaches rely on chemical interaction between an electron-rich nucleophile and  $CO_2$  to form some type of adduct. One of the best known approaches in this vein involves reaction of amines with  $CO_2$  to give carbamates.<sup>2</sup> This chemistry can be carried out in basic aqueous solutions containing amines, with amines immobilized onto various types of solid supports, or with other solid or liquid media containing amine groups, such as ionic liquids.<sup>2</sup> In most such cases the release of  $CO_2$  to recycle the capture agent requires heat. Few other chemistries have been described that enable reversible  $CO_2$  capture. Thus, there is interest in exploring new methods for  $CO_2$  capture. In addition, there is a broader need to more fully explore the chemistry of  $CO_2$ , and especially to explore the chemistry of compounds that form adducts with  $CO_2$ .

Several research efforts have explored approaches to capture  $CO_2$  using electrochemically generated nucleophiles. Mizen and Wrighton demonstrated that electrochemical reduction of quinones under aprotic conditions produces radical anions capable of  $CO_2$  capture at the quinone oxygen, producing aromatic carbonates.<sup>3</sup> They also showed that the resulting carbonates could be electrochemically oxidized, regenerating the quinone species and releasing  $CO_2$ . This stimulated a number of groups to explore  $CO_2$  capture using quinones.<sup>4–6</sup> In a related approach, release of amine ligands from Cu(II) amine complexes by electrochemical reduction to Cu metal can be used to drive  $CO_2$  capture via carbamate formation, connecting the traditional amine capture agent approach with the superior energetics inherent in electrochemical cycling.<sup>7</sup> In a recent report, we examined the reaction between 4,4'-bipyridine radical anion (which can be produced either electrochemically or photochemically) and carbon dioxide, demonstrating formation of a unique N-bound  $CO_2$  adduct species.<sup>8</sup> One electron oxidation of the adduct releases  $CO_2$  and regenerates 4,4'-bipyridine. All of these systems demonstrate chemically reversible electrochemical capture and release of  $CO_2$ . Their common theme is that electrochemical reduction of a precursor is employed to either directly generate or cause the release of a potent nucleophile that is capable of attacking the electrophilic carbon atom in  $CO_2$ , thereby forming an adduct. A subsequent oxidation process leads to  $CO_2$  release and regeneration of the precursor to the capture agent. For the quinone and bipyridine cases, release is accomplished by oxidation of the adduct itself.

We describe here a new chemistry for electrochemical  $CO_2$  capture and release that employs reduction of organic disulfide precursors to generate thiolate species that are potent nucleophiles toward  $CO_2$ . We show that benzylthiolate can bind  $CO_2$  to form a sulfur-bound thiocarbonate and that subsequent oxidation of the thiocarbonate leads to release of  $CO_2$  and regeneration of the disulfide. We are aware of only a few previous reports of *S*-bound terminal thiocarbonates,<sup>9–11</sup> and no previous reports of their electrochemical properties. In most of this study, the electrochemical capture and release of  $CO_2$  is pursued in ionic liquid (IL) media. A substantial literature exists on capture of  $CO_2$  using ILs containing amines and other nucleophilic functional groups.<sup>12</sup> Their low volatility

Received: October 15, 2016

Published: January 4, 2017



and suitability as electrochemical solvents makes ILs especially useful as supporting electrolytes in the present study. In some experiments we also employ dimethylformamide (DMF) as solvent, demonstrating the broader applicability of this chemistry to more traditional solvents. The reasonable solubilities of benzyldisulfide (BDS) in 1-butyl-1-methylpyrrolidinium bis(trifluoromethylsulfonyl)imide (BMP TFSI) and DMF (106 mM and 2 M, respectively) allow for facile electrochemical and synthetic experimentation.

Figure 1 shows a cyclic voltammogram (CV) of the reduction of BDS in BMP TFSI at a concentration of 20

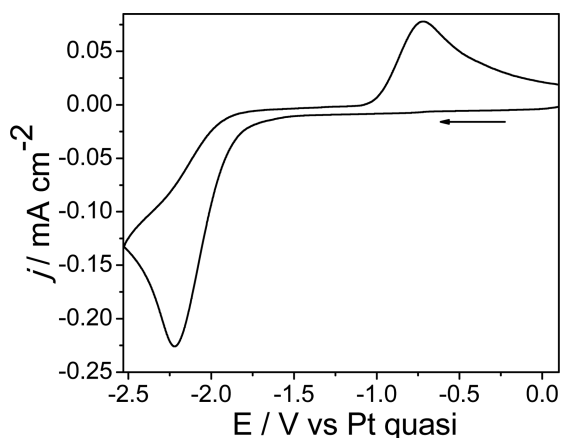


**Figure 1.** Cyclic voltammetry of 20 mM benzyldisulfide in BMP TFSI ionic liquid. Conditions: working, glassy carbon electrode; reference and counter, Pt electrode; scan rate, 10 mV/s.

mM. Reduction gives a well-formed voltammetric wave with a peak potential near  $-2.2$  V. This overall two-electron reduction process is as expected for reduction of organic disulfides, producing 2 equiv of the corresponding thiolate.<sup>13</sup> Oxidation of the benzylthiolate that is produced is seen on the return scan as an oxidation wave with a peak potential of  $-0.7$  V. The significant difference between the peak currents for disulfide reduction and thiolate oxidation is likely due to significant differences in diffusion coefficients for these two species. A similar phenomenon has been previously reported for the dioxygen/superoxide and ferrocene/ferrocenium redox couples in ILs, and attributed to significantly lower diffusion coefficients for charged species compared to neutrals.<sup>14,15</sup> The large peak separation between disulfide reduction and thiolate oxidation results from the fact that this redox mechanism is not microscopically reversible. We explored the mechanism of this process in some detail previously for a related disulfide/thiolate redox couple.<sup>16</sup> Briefly, reduction initially produces the  $\text{RSSR}^-$  radical anion. This species dissociates to produce 1 equiv each of  $\text{RS}^-$  and  $\text{RS}^\bullet$  (i.e., thiolate and thiyl radical).<sup>17</sup> The rapid electrochemical reduction of  $\text{RS}^\bullet$  produces a second equivalent of  $\text{RS}^-$ . On the subsequent positive-going scan, oxidation of the thiolate initially produces  $\text{RS}^\bullet$ , two of which rapidly couple to regenerate the parent disulfide. Subsequent work has confirmed the mechanistic aspects of this redox process, as well as providing more details about the nature of the dissociative electron transfer of the disulfides.<sup>18,19</sup> For the present purposes, a key feature of the disulfide reduction is that it produces thiolates, which are well known as potent nucleophiles and have been previously reported to react with  $\text{CO}_2$  to give S-bound thiocarbonates.<sup>9–11</sup>

Figure 2 shows the results of several experiments in 20 mM BDS in BMP TFSI in which the concentration of dissolved

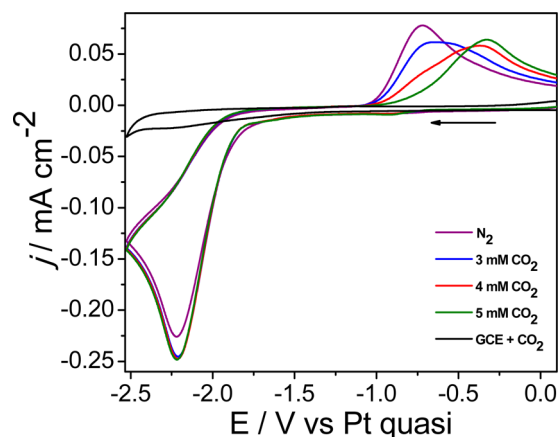


**Figure 2.** Cyclic voltammetry of 20 mM BDS in BMP TFSI IL with different concentrations of  $\text{CO}_2$ :  $\text{N}_2$  (purple), 3 mM  $\text{CO}_2$  (blue), 4 mM  $\text{CO}_2$  (red), 5 mM  $\text{CO}_2$  (green), 100 mM  $\text{CO}_2$  in the absence of BDS in IL (black), Conditions: working, GCE; reference and counter, Pt electrode; scan rate, 10 mV/s.

$\text{CO}_2$  was serially increased by increasing the  $\text{CO}_2$  partial pressure in a purging gas stream comprising a mixture of  $\text{N}_2$  and  $\text{CO}_2$ . As  $[\text{CO}_2]$  is increased, the benzylthiolate oxidation peak at  $-0.7$  V is decreased. At the same time, a new oxidation peak appears at  $-0.3$  V. As will be shown further below, this new oxidation peak corresponds to oxidation of S-benzylthiocarbonate,  $\text{RSCO}_2^-$ . This is the first report of electrochemical behavior for a terminal S-bound thiocarbonate species. Figure 2 also shows a background CV at a glassy carbon electrode (GCE) in pure BMP TFSI at 100 mM  $\text{CO}_2$  but containing no BDS, demonstrating that  $\text{CO}_2$  is electrochemically inactive at glassy carbon over the potential range shown in the CV. For comparison, Figure S7 shows the chemically irreversible reduction of  $\text{CO}_2$  at Au over this same range of potentials, demonstrating a large reduction peak for  $\text{CO}_2$  at  $-2.3$  V. The lack of  $\text{CO}_2$  electroactivity at a GCE over this potential range is likely due to the absence of strong adsorption at this surface. We take advantage of this lack of reactivity to explore the interactions between thiolates and  $\text{CO}_2$  without interference by direct  $\text{CO}_2$  reduction. The observation that 5 mM  $\text{CO}_2$  is sufficient to completely eliminate the oxidation response from 40 mM benzylthiolate (produced by reduction of 20 mM BDS) is attributed to the much faster diffusion of  $\text{CO}_2$  than benzylthiolate in the IL, similar to the discussion above regarding dissimilar diffusion coefficients.<sup>14,15</sup> In other words, the rapid diffusive transport of  $\text{CO}_2$  to the region near the electrode allows a 5 mM  $\text{CO}_2$  solution to provide sufficient  $\text{CO}_2$  to completely consume the higher concentration of electrochemically generated thiolate through formation of the thiocarbonate.

The reversibility of the uptake of  $\text{CO}_2$  by thiolate and release by thiocarbonate oxidation was also examined. Figures S8 and S9 show that the new thiocarbonate oxidation peak at  $-0.3$  V can be caused to appear or disappear simply by purging a BDS solution in BMP TFSI with a  $\text{CO}_2$ -rich or  $\text{N}_2$ -rich gas stream, respectively, prior to a cyclic voltammetric scan over the disulfide reduction wave. This shows that the  $\text{CO}_2$  capture-and-release cycle is chemically reversible under the conditions of these experiments. Figure S10 shows the scan rate dependence

of the capture–release cycle at a concentration of CO<sub>2</sub> sufficiently high to consume all of the thiolate produced during the reduction. The discussion of the figure in the [Supporting Information](#) provides the mechanistic details of the adduct formation, revealing that it is not a simple EC type of mechanism due to the complexity of the RSSR reduction pathway.<sup>20</sup>

In order to show that the oxidation peak at −0.3 V is caused by a thiocarbonate species, the voltammograms of authentic samples of benzylthiolate and *S*-benzylthiocarbonate were directly compared. [Figure 3](#) shows the results of cyclic

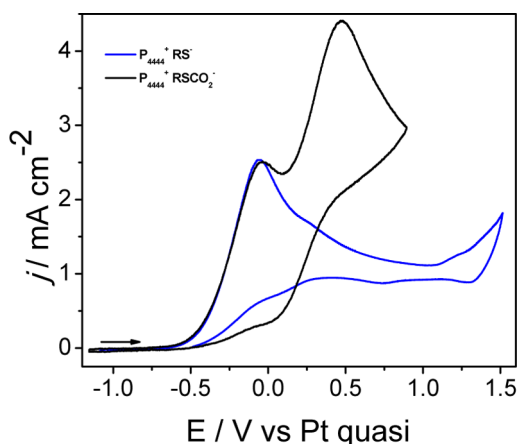


**Figure 3.** Cyclic voltammetry of 30 mM P<sub>4444</sub><sup>+</sup> RS<sup>−</sup> (blue) and 30 mM P<sub>4444</sub><sup>+</sup> RSCO<sub>2</sub><sup>−</sup> (black) in 0.1 M TBAP in DMF. Conditions: working, GCE; reference and counter, Pt electrode; scan rate, 50 mV/s.

voltammetric experiments in which authentic samples of the P<sub>4444</sub><sup>+</sup> salts of benzylthiolate and *S*-benzylthiocarbonate were sequentially added to DMF supporting electrolyte in equimolar amounts. Preparation and characterization of these samples are described in the [Supporting Information](#). As can be seen, the two species exhibit different oxidation potentials. The benzylthiolate oxidation peak is observed at −0.1 V. The *S*-benzylthiocarbonate oxidation peak is observed at +0.4 V, shifted in the positive direction by 0.5 V compared to the thiolate oxidation peak. [Figure S11](#) shows the CV for an equimolar solution of the P<sub>4444</sub><sup>+</sup> salts of benzylthiolate and *S*-benzylthiocarbonate in P<sub>4444</sub> TFSI. Again, one can see that the two species are oxidized at different potentials, though the broadness of the peaks in this much higher viscosity IL makes the individual responses less resolvable. The results in [Figures 3](#) and [S11](#) are consistent with the interpretation that the new oxidation observed in [Figure 2](#) when CO<sub>2</sub> is dissolved into the IL solution is due to the appearance of a thiocarbonate species that is more difficult to oxidize than the thiolate.

To further demonstrate uptake and release of CO<sub>2</sub> for this system, we performed bulk electrolysis experiments in which purge gases were swept through the cell to monitor CO<sub>2</sub> uptake and release using a nondispersive CO<sub>2</sub> gas sensor downstream from the cell. In [Figure S12](#) we show the results of a reductive bulk electrolysis of BDS in the presence of a flowing stream of 350 ppm of CO<sub>2</sub> in N<sub>2</sub>. The figure shows that CO<sub>2</sub> in the purge gas stream is completely consumed when reductive current is passed in the working electrode chamber, which produces benzylthiolate that subsequently reacts with CO<sub>2</sub>. In [Figure S13](#) we show the results of a quantitative oxidative bulk electrolysis of a sample of *S*-benzylthiocarbonate. In this experiment, we

monitor the evolution of CO<sub>2</sub> during oxidation by sweeping it from the cell in a stream of pure N<sub>2</sub> and detecting it downstream. The right plot in the figure shows that moles of e<sup>−</sup> (from the oxidative charge) and moles of CO<sub>2</sub> released (from integration of the sensor signal) are equal within experimental error. Except for a short lag time due to the transit time to the detector, the CO<sub>2</sub> release is seen to be coincident with the accumulation of oxidative charge. This plot shows clearly that CO<sub>2</sub> release in this experiment is due to oxidation of the thiocarbonate, and that 1 equiv of CO<sub>2</sub> is released for each equivalent of oxidative charge. Taken together, the results confirm that electrochemical generation of benzylthiolate in the presence of CO<sub>2</sub> produces *S*-benzylthiocarbonate. Oxidation of this thiocarbonate releases CO<sub>2</sub> and regenerates the disulfide, which can be observed on the following negative-going scan via its reduction, as evidenced by the continuous scans in [Figures S8](#) and [S9](#). These observations show that oxidation of a terminal *S*-bound thiocarbonate is similar to the well-known Kolbe oxidation of organic carboxylates, where oxidation results in decarboxylation.<sup>21</sup> Thus, these results are consistent with the electrochemical capture and release of CO<sub>2</sub> as mediated by the disulfide/thiocarbonate redox couple.

Quantum chemical calculations at the B3LYP/aug-cc-pVQZ level were also used to understand the nature of the interaction between the thiolate and CO<sub>2</sub> and the stability of the thiocarbonate. [Figure 4](#) shows the results of such a calculation

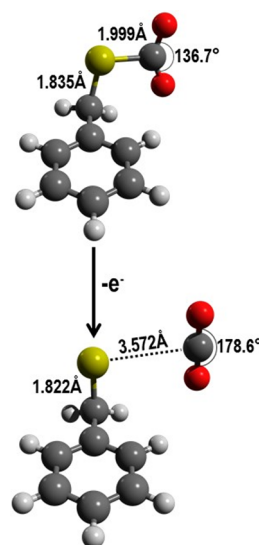


**Figure 4.** Quantum mechanical calculation of *S*-benzylthiocarbonate done at B3LYP/aug-cc-pVQZ level. Atoms: S (yellow), O (red), H (light gray), C (dark gray).

done at the B3LYP/aug-cc-pVQZ level on *S*-benzylthiocarbonate. Calculations at this level of theory were found to yield good agreement with experimental enthalpies of sulfur-containing compounds.<sup>22</sup> The figure shows the minimized geometry of the thiocarbonate (upper structure). The C–S bond length is 1.999 Å, and the calculated B3LYP/aug-cc-pVDZ enthalpy for the binding of CO<sub>2</sub> to the thiolate is −66.3 kJ/mol. This enthalpy for binding shows formation of a stable *S*-bound terminal thiocarbonate for this case. These respective quantities are within the range expected for C–S single bonds and for other stable CO<sub>2</sub> adducts.<sup>23–26</sup> The OCO bond angle of 136.7° indicates considerable rehybridization around carbon resulting from strong interaction with the sulfur center. Thus,



the quantum chemical calculations support the formation of a stable S-bound thiocarbonate from the reaction between benzylthiolate and CO<sub>2</sub>.

Figure 4 also shows the minimized geometry of the thiocarbonate after removal of one electron. The S–CO<sub>2</sub> bond length is dramatically elongated, at 3.572 Å, and the O–C–O bond angle is increased to 178.6°. These values confirm that there is essentially no bonding interaction of the CO<sub>2</sub> moiety with the S atom after oxidation, consistent with the release of CO<sub>2</sub> after oxidation. Figure S14 shows the HOMO and HOMO–1 electron density maps for the thiocarbonate. These orbitals are quasi-degenerate,<sup>27,28</sup> and show significant bonding electron density between the S atom and the carboxylate C atom. Thus, one electron oxidation should lead to destabilization of the S–C bond. This is similar to C–C bond cleavage leading to decarboxylation in Kolbe oxidation products, such as H<sub>3</sub>CCO<sub>2</sub><sup>•</sup>, the acetyloxyl radical.<sup>29</sup> In summary, these computational studies support the experimental results showing the formation of a stable terminal thiocarbonate from reaction of benzylthiolate and CO<sub>2</sub>. They also show that thiocarbonate oxidation results in cleavage of the S–CO<sub>2</sub> bond, producing a benzyl thiyl radical (two of which will then couple to form disulfide) and free CO<sub>2</sub>. This is similar to the oxidative dissociation of CO<sub>2</sub> previously reported for the adduct between the 4,4'-bipyridine radical anion and CO<sub>2</sub>, where oxidation from the HOMO leads directly to N–C bond scission and release of 4,4'-bipyridine and CO<sub>2</sub>.<sup>8</sup> More extensive calculations on a range of benzyl and phenyl thiocarbonate derivatives, to be reported elsewhere, reveal that the energy for binding of CO<sub>2</sub> to the RS<sup>•</sup> species depends on the electron density on the sulfur atom in RS<sup>•</sup>, implying that the enthalpy of CO<sub>2</sub> binding can be tuned through judicious choice of structural features on RS<sup>•</sup>.

We have demonstrated a completely new type of chemically reversible, electrochemical process for capture and release of CO<sub>2</sub> based on an organic disulfide/thiocarbonate redox couple. These data also comprise the first report of the electrochemical behavior for terminal S-bound thiocarbonates. Quantum chemical calculations are consistent with the capture of CO<sub>2</sub> by RS<sup>•</sup>, producing a stable thiocarbonate, and release of CO<sub>2</sub> after oxidation of the thiocarbonate. Additional experiments are underway to explore CO<sub>2</sub> separations based on this chemistry.

## ■ ASSOCIATED CONTENT

### Supporting Information

The Supporting Information is available free of charge on the ACS Publications website at DOI: 10.1021/jacs.6b10806.

Experimental details and characterization data, including Figures S1–S14 (PDF)

## ■ AUTHOR INFORMATION

### Corresponding Author

\*dan.buttry@asu.edu

### ORCID

Daniel A. Buttry: 0000-0002-6915-6914

### Notes

The authors declare no competing financial interest.

## ■ ACKNOWLEDGMENTS

We are grateful to the Department of Energy for support of this work through ARPA-E Contract DEAR0000343. J.H.R. was

supported by a National Science Foundation graduate fellowship.

## ■ REFERENCES

- (1) Kenarsari, S. D.; Yang, D. L.; Jiang, G. D.; Zhang, S. J.; Wang, J. J.; Russell, A. G.; Wei, Q.; Fan, M. H. *RSC Adv.* **2013**, *3*, 22739.
- (2) Dutcher, B.; Fan, M. H.; Russell, A. G. *ACS Appl. Mater. Interfaces* **2015**, *7*, 2137.
- (3) Mizen, M. B.; Wrighton, M. S. *J. Electrochem. Soc.* **1989**, *136*, 941.
- (4) Scovazzo, P.; Poshusta, J.; DuBois, D.; Koval, C.; Noble, R. J. *Electrochem. Soc.* **2003**, *150*, D91.
- (5) Gurkan, B.; Simeon, F.; Hatton, T. A. *ACS Sustainable Chem. Eng.* **2015**, *3*, 1394.
- (6) Apaydin, D. H.; Glowacki, E. D.; Portenkirchner, E.; Sariciftci, N. S. *Angew. Chem., Int. Ed.* **2014**, *53*, 6819.
- (7) Stern, M. C.; Hatton, T. A. *RSC Adv.* **2014**, *4*, 5906.
- (8) Ranjan, R.; Olson, J.; Singh, P.; Lorange, E. D.; Buttry, D. A.; Gould, I. R. *J. Phys. Chem. Lett.* **2015**, *6*, 4943.
- (9) Stueber, D.; Grant, D. M. *Solid State Nucl. Magn. Reson.* **2002**, *22*, 439.
- (10) Stueber, D.; Orendt, A. M.; Facelli, J. C.; Parry, R. W.; Grant, D. M. *Solid State Nucl. Magn. Reson.* **2002**, *22*, 29.
- (11) Stueber, D.; Patterson, D.; Mayne, C. L.; Orendt, A. M.; Grant, D. M.; Parry, R. W. *Inorg. Chem.* **2001**, *40*, 1902.
- (12) Cui, G. K.; Wang, J. J.; Zhang, S. J. *Chem. Soc. Rev.* **2016**, *45*, 4307.
- (13) Liu, M. L.; Visco, S. J.; Dejonghe, L. C. *J. Electrochem. Soc.* **1989**, *136*, 2570.
- (14) Buzzeo, M. C.; Klymenko, O. V.; Wadhawan, J. D.; Hardacre, C.; Seddon, K. R.; Compton, R. G. *J. Phys. Chem. A* **2003**, *107*, 8872.
- (15) Barrosse-Antle, L. E.; Bond, A. M.; Compton, R. G.; O'Mahony, A. M.; Rogers, E. I.; Silvester, D. S. *Chem. - Asian J.* **2010**, *5*, 202.
- (16) Shouji, E.; Buttry, D. A. *J. Phys. Chem. B* **1999**, *103*, 2239.
- (17) Hoffman, M. Z.; Hayon, E. *J. Am. Chem. Soc.* **1972**, *94*, 7950.
- (18) Antonello, S.; Daasbjerg, K.; Jensen, H.; Taddei, F.; Maran, F. *J. Am. Chem. Soc.* **2003**, *125*, 14905.
- (19) Meneses, A. B.; Antonello, S.; Arevalo, M. C.; Gonzalez, C. C.; Sharma, J.; Wallethe, A. N.; Workentin, M. S.; Maran, F. *Chem. - Eur. J.* **2007**, *13*, 7983.
- (20) Batchelor-McAuley, C.; Compton, R. G. *J. Electroanal. Chem.* **2012**, *669*, 73.
- (21) Utley, J. *Chem. Soc. Rev.* **1997**, *26*, 157.
- (22) Tian, Z. X.; Pawlow, A.; Poutsma, J. C.; Kass, S. R. *J. Am. Chem. Soc.* **2007**, *129*, 5403.
- (23) D'Alessandro, D. M.; Smit, B.; Long, J. R. *Angew. Chem., Int. Ed.* **2010**, *49*, 6058.
- (24) Heldebrant, D. J.; Yonker, C. R.; Jessop, P. G.; Phan, L. *Energy Environ. Sci.* **2008**, *1*, 487.
- (25) Koh, H. S.; Rana, M. K.; Hwang, J.; Siegel, D. J. *J. Phys. Chem. Chem. Phys.* **2013**, *15*, 4573.
- (26) Lee, H. M.; Youn, I. S.; Saleh, M.; Lee, J. W.; Kim, K. S. *Phys. Chem. Chem. Phys.* **2015**, *17*, 10925.
- (27) Boixel, J.; Blart, E.; Pellegrin, Y.; Odobel, F.; Perin, N.; Chiorboli, C.; Fracasso, S.; Ravaglia, M.; Scandola, F. *Chem. - Eur. J.* **2010**, *16*, 9140.
- (28) Pistner, A. J.; Pupillo, R. C.; Yap, G. P. A.; Lutterman, D. A.; Ma, Y. Z.; Rosenthal, J. J. *J. Phys. Chem. A* **2014**, *118*, 10639.
- (29) Rauk, A.; Yu, D.; Armstrong, D. A. *J. Am. Chem. Soc.* **1994**, *116*, 8222.